Tetrahedron 69 (2013) 5874–5879

Contents lists available at SciVerse ScienceDirect

Tetrahedron

journal homepage: www.elsevier.com/locate/tet

Ratiometric pH responsive fluorescent probes operative on ESIPT

Yim-Pan Chan [a], Li Fan [a,b], Qihua You [a], Wing-Hong Chan [a,*], Albert W.M. Lee [a], Shaomin Shuang [b]

[a] Department of Chemistry, Hong Kong Baptist University, Kowloon Tong, Hong Kong Special Administrative Region
[b] Center of Environmental Science and Engineering Research, School of Chemistry and Chemical Engineering, Shanxi University, Taiyuan 030006, PR China

ARTICLE INFO

Article history:
Received 22 January 2013
Received in revised form 22 April 2013
Accepted 10 May 2013
Available online 16 May 2013

Keywords:
Spirobenzopyran
pH sensing
Ratiometric fluorescent probe
ESIPT

ABSTRACT

A series of C-8′-oxime-appended spirobenzopyrans **4a**–**4d** were synthesized and developed as fluorescent pH ratiometric probes operative in HEPES/ACN (8:2, v/v) buffer solutions. Acidochromic conversion of spirobenzopyran to merocyanine open form can facilitate the subsequent enol–keto tautomerization giving dual emissive peaks via the excited state intramolecular proton transfer (ESIPT) mechanism. The pH titrations of **4a** show a 68-fold increase in ratiometric intensities ratio ($I_{645\ nm}/I_{522\ nm}$) when the pH was switched from 8.0 to 4.0 with a pK_a value of 5.90.

1. Introduction

Owing to their intrinsic simplicity and selectivity, fluorescent probes are versatile tools for visualizing and detecting metal cations, anions, and biologically relevant small organic molecules.[1–3] Measurement of pH by fluorescence-based techniques has important implications in analytical and biological chemistry. Development of fluorescent pH sensing probes for both imaging and sensing applications has received much attention in the current literature.[4] Probes characterized by their ratiometric and 'off–on' signal outputs in response to physiological pH variations are widely sought after sensing devices. A handful of detection schemes exploiting proton binding induced perturbations of de-excitation pathways such as photo-induced electron transfer (PET),[4a,b] intramolecular charge transfer (ICT),[4e] Forster resonance energy transfer (FRET)[4c,d] have been used for the development of pH sensing probes.

Recently, excited state intramolecular proton transfer (ESIPT) has emerged as an effective fluorescent signal transduction mechanism for designing novel ratiometric fluorescent probes. For instance, operating on ESIPT, fluorescent probes for Hg(II), pyrophosphate, and cysteine have been established in the literature.[5] In recent years, spirobenzopyrans were chosen by us as the molecular scaffold for developing novel fluorescent chemosensors for Cu^{2+}, Zn^{2+}, pyrophosphate, and glutathione.[6] Analyte induced conversion of the non-fluoresced spirobenzopyran close form to fluoresced merocyanine open form contributed to the basis for the turn-on sensor development. It is also well known that such a transformation can be achieved by acidification of spirobenzopyran derivatives.[7]

The present report is directed toward the synthesis and fluorimetric characterization of spirobenzopyran derivatives **4a**–**4d** possessing tunable pK_a values close to the physiological pH range that can detect the pH changes of aqueous solutions. Operating on the ESIPT mechanism, the probes in response to pH variations afforded ratiometric fluorescent signals originated from the enol- and keto-tautomer, respectively.

2. Results and discussion

Acidochromic ring opening of spirobenzopyran affords the corresponding merocyanine bearing a phenolic moiety. By incorporating an oxime moiety onto the C-8′ of the spirobenzopyran skeleton, the merocyanine derivatives formed under acidic conditions will possess a molecular platform, which can undergo intramolecular proton transfer from the phenolic oxygen to the oxime nitrogen in the photo-excited state as shown in Scheme 1.

Our rational design of spirobenzopyran-based fluorescent pH probes possesses two attractive features. The pH responsive characteristics of the probes can be tuned by incorporating of different substituents onto the benzene ring. Upon acidification and excitation, the enol produced at its excited state could undergo tautomerization gives rise to an emission with large Stokes' shift. In

* Corresponding author. Tel.: +852 34117076; fax: +852 34117348; e-mail address: whchan@hkbu.edu.hk (W.-H. Chan).

0040-4020/$ – see front matter © 2013 Elsevier Ltd. All rights reserved.
http://dx.doi.org/10.1016/j.tet.2013.05.023

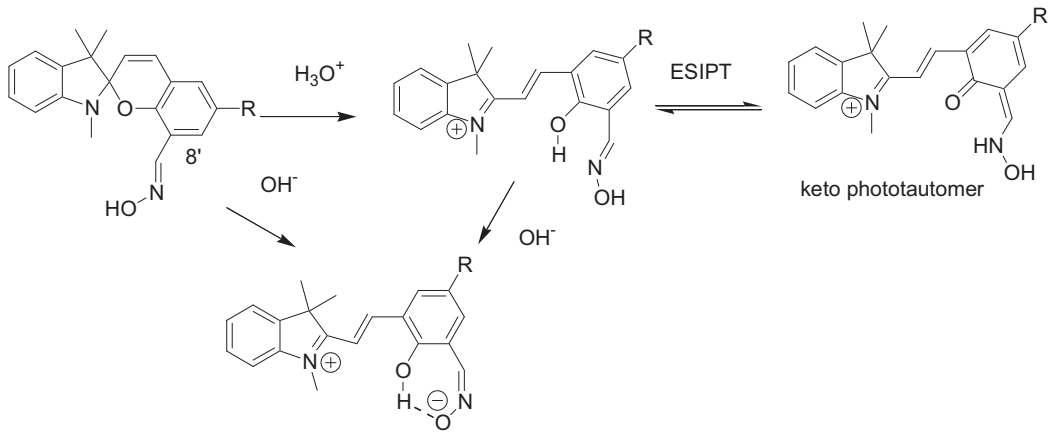

Scheme 1. Acid induced conversion of spirobenzopyran to merocyanine undergoing ESIPT.

essence, the dual normal and ESIPT de-excitation pathway would give two emissive peaks as ratiometric output signals.

The syntheses of 6′-subsituted 8′-oxime-appended spirobenzopyrans **4a**–**4d** were carried out efficiently in a three-step reaction sequence starting from the respective 4-substitued phenol shown in Scheme 2. Using the literature protocol, clean diformylation of *p*-substituted phenols **1a**–**1d** was accomplished by reaction with 2 equiv of hexamethylenetetramine in refluxing trifluoroacetic acid, affording the corresponding dialdehydes **2a**–**2d**, respectively.[8] Subsequent treatment of the dialdehydes with 1 equiv of hydroxylamine hydrochloride salt in the presence of 1 equiv of NaOH gave the corresponding mono-oximes **3a**–**3d**, respectively, in 31–51% yield. Good yield of **4a**–**4d** was obtained by heating the mono-oximes separately with 1.2 equiv of *N*-methyl-2,3,3-trimethylindolenine iodide and morpholine in absolute ethanol.[9]

centered at 385 and 425 nm as shown in Fig. 1A. In alkali conditions, a new absorption peak at 550 nm with low intensity emerges with a clear isosbestic point at 500 nm. The observed red-shifted absorption peak could be due to the intramolecular charge transfer of the ring open merocyanine form taking place in the ground state. It is noteworthy that, in contrast to other substituted spirobenzopyrans, the presence of the oxime hydroxyl moiety may stabilize the phenoxyl group preventing its cyclization back to the close form. To substantiate this presumption, a control compound **5** was synthesized by alkylating the oxime hydroxyl group with benzyl chloride (Fig. S1). The UV–vis spectra of **5** at different pH revealed that the merocyanine open form of **5** underwent ring closure to the spirobenzopyran close form at alkali solutions (Fig. S2).

The fluorescence spectra of **4a** excited at 425 nm in HEPES/ACN buffer solutions of pH 3.0–9.0 were recorded. In pH=9.0, **4a** ex-

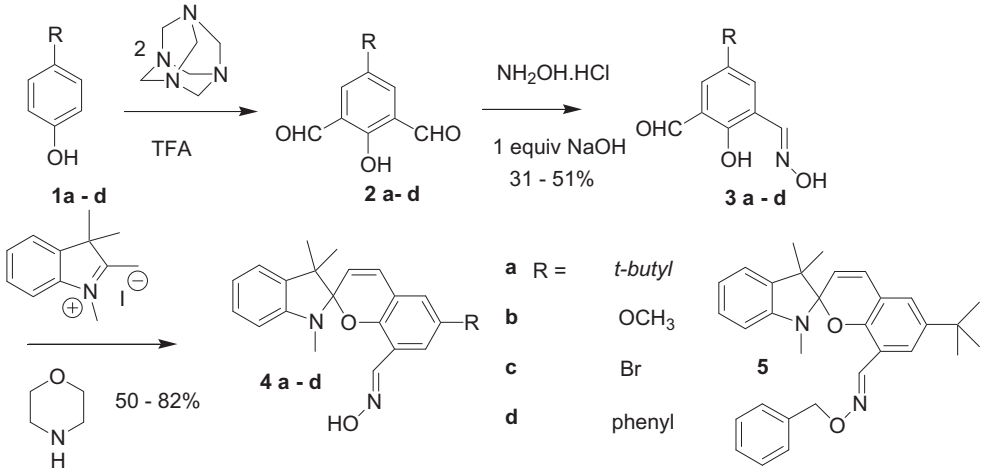

Scheme 2. Synthetic route to the fluorescent pH sensing probes and the structure of control compound **5**.

With the fluorescent sensory materials in hand, we explored their use as fluorescent pH sensing probes. On the outset of the investigation, for practical reason, we chose 8:2 aqueous buffered acetonitrile solution as the solvent for studying the pH responsive properties of the probes. The spectroscopic properties of **4a** were first selected to be examined under different pH conditions. The acidochromic interconversion of the spirobenzopyran close form of **4a** to the extended conjugated merocyanine ring open form was evidenced from its UV–vis absorption spectra obtained from different HEPES buffer solutions. Under strong acidic conditions, **4a** exhibits two typical π–π^* partially overlapped absorption bands hibits only one emissive peak at 522 nm. With an increase in pH, its fluorescence intensity at 522 nm was reduced and a new emission band at 645 nm emerged concomitantly. The band at higher energy could be attributed to the emission from hydrogen bonded enol tautomer. The large Stokes' shifted emission band at λ_{em}=645 nm can conceivably be assigned to the keto-tautomer form in excited state from the enol-tautomer (Scheme 1). The phototautomer possessing short life time (i.e., in picosecond) emits long wave light and back to the ground state.[10] Apparently, the pH variation triggers the display of ratiometric fluorescence signal changes from **4a**. A clear isoemission point is apparent at 590 nm, which indicated the

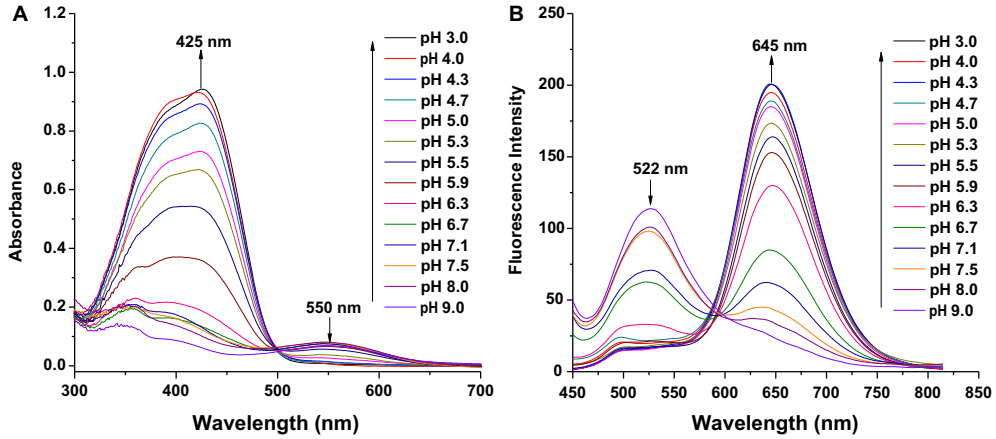

Fig. 1. UV–vis absorption (A) and fluorescence emission spectra (B) of **4a** (50 μM) at different pH values in HEPES buffer/ACN (8:2, v/v) with λ_{ex}=425 nm.

equilibrium between the keto and the enol form. A plot of the ratios of the emission intensities of **4a** at 645 and 522 nm against the pH of the solutions is shown in Fig. 2, displaying the typical sigmoidal relationship between the two parameters (R^2=0.995). This intensities ratio decreased from 13.48 to 0.20 associated with pH change from 3.0 to 9.0, giving a huge value change of 68 between two plateaus of the pH titration curve. Non-linear curve fitting using Boltzmann equation, on the basis of the plot of fluorescence intensities ratios against pH, the pK_a of the probe was calculated to be 5.90.[4d] The typical application range of **4a** can be estimated to be 4.0–8.0. Additionally, the probe displayed a fast response time toward the pH change of the solutions. As shown in Fig. S3, stable and steady fluorescent readings can be obtained within 6 min.

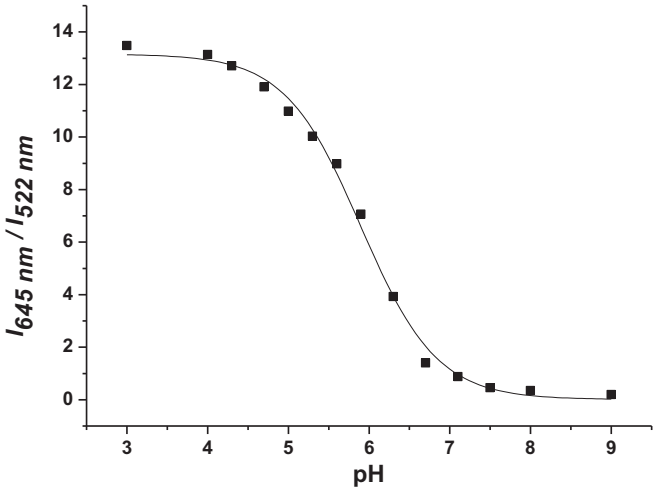

Fig. 2. Plot of the emission intensities ratios of R at $I_{645\ nm}/I_{522\ nm}$ to pH variation in HEPES buffer/ACN (8:2, v/v) with λ_{ex}=425 nm.

To define the application scope of this pH probe, its response to other common metal ions should be examined. To investigate this phenomenon, metal ion selectivity assays were conducted at both pH 4.0 and 7.0. Upon addition of 2400 equiv (120 mM) of Na^+, K^+ to **4a** solution, no change in its fluorescence was observed at both pH values. Furthermore, adding 6 equiv of other 12 common metal ions (0.3 mM), i.e., Li^+, Ca^{2+}, Mg^{2+}, Fe^{2+}, Fe^{3+}, Zn^{2+}, Co^{2+}, Ni^{2+}, Cd^{2+}, Hg^{2+}, Pb^{2+}, Ag^+ separately into **4a** solution did not cause any adverse effect on the ratios of emission intensities of the probe, and the ratios remained almost constant at pH 4.0 and 7.0, respectively (Fig. 3). The interference studies further revealed that only Cu^{2+} exhibited substantial quenching effect on the fluorescence output signals of **4a**, irrespective of the pH of the solution. The interference results imply that **4a** can selectively measure pH in the presence of various metal ions usually present in biological systems. Furthermore, the significant interference effect caused by Cu^{2+}can be

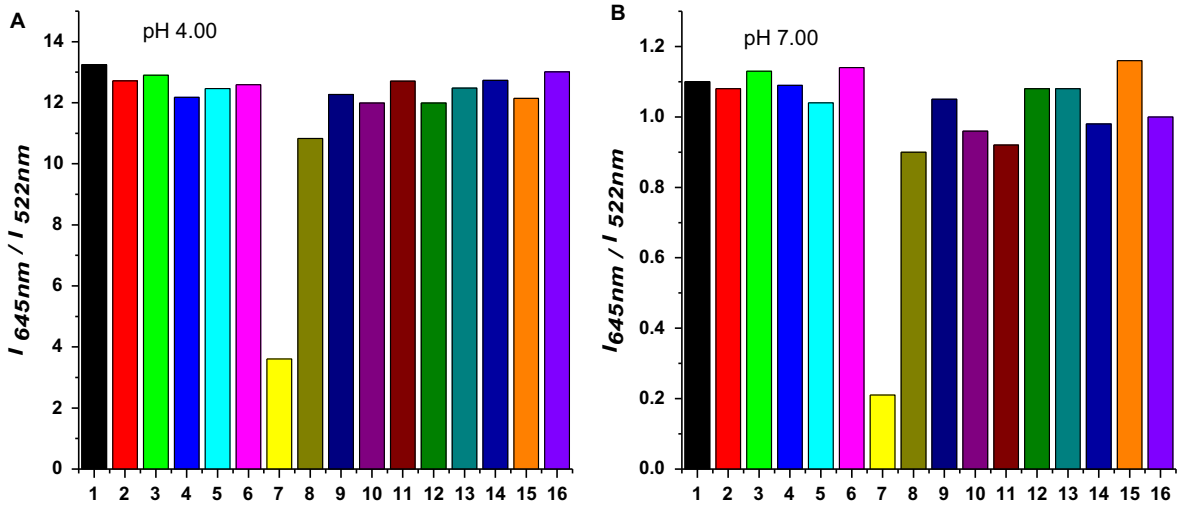

Fig. 3. Metal ion selectivity profiles of **4a**—emission ratios ($I_{645\ nm}/I_{522\ nm}$) of **4a** (50 μM) in 80% HEPES/ACN [50 mM, pH=4.00 (A) and pH=7.00 (B)]. λ_{ex}=425 nm, slit=10/10 nm. 1, free; 2, Li^+ (0.3 mM); 3, Na^+ (120 mM); 4, K^+ (120 mM); 5, Ca^{2+} (0.3 mM); 6, Mg^{2+} (0.3 mM); 7, Cu^{2+} (0.3 mM); 8, Fe^{3+} (0.3 mM); 9, Fe^{2+} (0.3 mM); 10, Zn^{2+} (0.3 mM); 11, Co^{2+} (0.3 mM); 12, Ni^{2+} (0.3 mM); 13, Cd^{2+} (0.3 mM); 14, Ag^+ (0.3 mM); 15, Hg^{2+} (0.3 mM); and 16, Pb^{2+} (0.3 mM).

conveniently removed by using *o*-ethylxanthic acid as the screening agent. As shown in Fig. S4, the quenching effect on the probe caused by Cu^{2+} (0.3 mM) in both pH 4.00 and 7.00 buffered solutions can be eliminated by the addition of a same amount of *o*-ethylxanthic acid.

It is our intention to design and synthesize a series of potential pH fluorescent probes possessing tunable pK_a values. The nature of substituents appended at the C-6′ position of spirobenzopyrans could affect the photophysical properties of the materials. Therefore, using the same synthetic protocol outlined in Scheme 1, spirobenzopyrans **4b**, **4c**, and **4d** were synthesized for comparative investigation. Starting from the corresponding 4-substituted phenol, all these three compounds can be obtained in moderate overall yield. Their structures were fully characterized by NMR and HRMS spectroscopy. Their optical characteristics in response to pH change were established by UV–vis and fluorescence spectroscopy. UV–vis absorption spectral changes of **4b** and **4c** in aqueous ACN solution at different pH values are shown in Fig. S5. To assess their applicability as pH fluorescent sensing probes, their fluorescent spectra in 8:2 HEPES buffer and ACN (v/v) at different pH were measured and are shown in Fig. 4. To certain extent, the photophysical properties of these three analogs of **4a** are very similar. Dual fluorescence outputs were observed at different pH solutions. Apparently, the rapid process of enol–keto tautomerization as a result of ESIPT took place for all these materials under acidic conditions. Evidently, compounds **4a**–**4d** are suitable materials for the development of ratiometric pH fluorescent probes.

Careful examination of the fluorescence data of these materials revealed that different substituents appended at the C-6′ of spirobenzopyran scaffold would cause some subtle changes of photophysical properties of the resultant compounds. However, the ratio between the dual fluorescence intensities of the four spirobenzopyrans correlated nicely with the pH values of the solutions (Fig. 5). Acting as ratiometric pH fluorescent probes, the pH dynamic working range and the response sensitivity of the probes are structurally dependent. Compound **4d** with a C-6′ substituted phenyl group exhibited the highest sensitivity to the pH variation of the solution. Under pH 4.0 and 9.0, a large difference of 175-fold in intensities ratio was recorded for **4d**. On the other hand, **4b** with a C-6′ substituted electron donating methoxy group displays the smallest separation in intensities ratio under the acidic and basic conditions.

For clear comparison of the photophysical properties of the materials, relevant properties of this series of compounds are compiled in Table 1. The exact position of the emission bands of the probes is strongly substituent-dependent. The presence of C-6′-methoxy group in the spirobenzopyran induced the greatest red-shift for both emissive peaks. On the basis of curve fitting, the pK_a found for these four probes is distinctive different ranging from 5.26 to 6.32. The phenyl group is most effective to enhance the acidity of the probe while strong electronic donating methoxy group reduced considerably the acidity of the probe. According to the quantum yield measurement, all synthesized materials are only modestly fluoresced under both acidic and basic aqueous conditions.

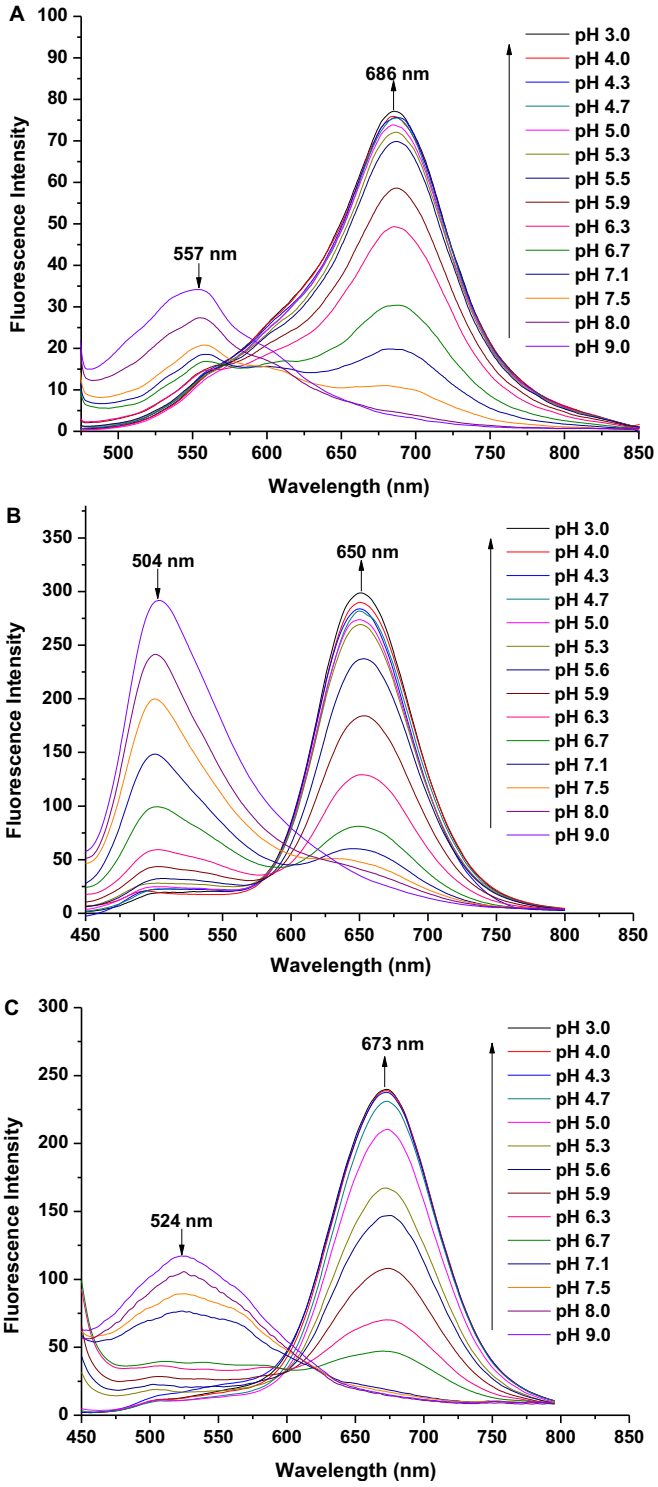

Fig. 4. The fluorescence emission spectra of (A) **4b**, (B) **4c** and (C) **4d**; (all in 50 μM) at different pH values in HEPES buffer/ACN (8:2, v/v) with λ_{ex}=425 nm.

3. Conclusion

In summary, we have successfully designed and synthesized a series of C-6′ substituted C-8′ oxime-appended spirobenzopyrans. The dual fluorescence outputs of all these materials were demonstrated to be pH dependent in aqueous solutions. The pK_a of the probes could be tuned by changing the substituent pattern at C-6′ of the molecules. The cross interference caused by common metal ions except Cu^{2+} to the pH probes is negligible.

4. Experimental section

4.1. General

The melting point was determined with a MEL-TEMPII melting point apparatus (uncorrected). ^{1}H NMR and ^{13}C NMR spectra were recorded on Bruker Advance-III 400 spectrometer (at 400 and

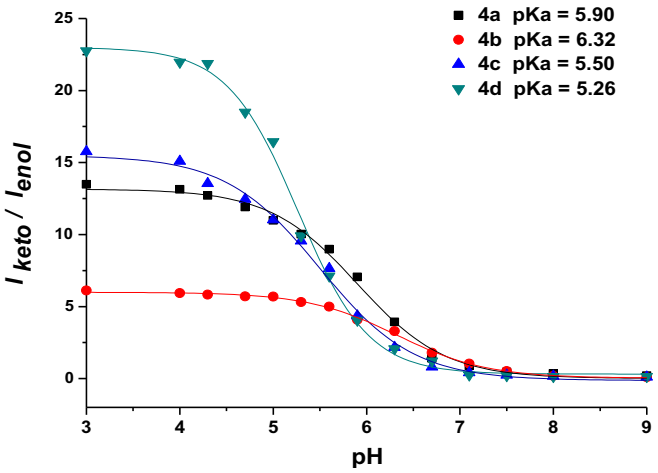

Fig. 5. Plots of the emission intensities ratios (i.e., I_{keto}/I_{enol}) of different probes to pH variation in HEPES buffer/ACN (8:2, v/v) with λ_{ex}=425 nm.

4.3. 5-(*tert*-Butyl)-2-hydroxy-3-((hydroxyimino)methyl)benzaldehyde (3a)

A solution of 5-(*tert*-butyl)-2-hydroxyisophthalaldehyde (1.085 g, 5.36 mmol) in ethanol (50 mL) was mixed with a solution of hydroxylamine hydrochloride (366 mg, 5.36 mmol) and sodium hydroxide (25 mg). The reaction mixture was heated to 60 °C for overnight. After being cooled to room temperature, part of solvent was removed under reduced pressure. Then the reaction mixture was diluted with water and extracted with ethyl acetate (3×50 mL). The combined organic layers were dried by anhydrous sodium sulfate and filtered. The filtrate was evaporated under vacuum to afford a crude residue that was purified by column chromatography (*n*-hexane/ethyl acetate 50:1) to yield product **3a** (441 mg, 38% yield) as pale yellow oil. H NMR ($CDCl_3$-d_1) δ (ppm): 1.33 (s, 9H), 7.68 (d, 1H, *J*=2.4 Hz), 7.81 (d, 1H, *J*=2.4 Hz), 8.44 (s, 1H), 9.19 (br s, 1H), 10.10 (s, 1H), 11.09 (s, 1H). C NMR ($CDCl_3$-d_1) δ (ppm): 31.2, 34.2, 119.3, 121.5, 130.2, 132.5, 142.9, 147.8, 157.8, 194.6.

Compounds **3b**, **3c**, and **3d** were prepared using the same procedure.

Table 1
Photophysical properties of the spirobenzopyran derivatives in HEPES buffer/ACN (8:2, v/v) solutions

Probe	λ_{abs} (nm)	ε (10^4 M^{-1} cm^{-1})	λ_{em} (nm)	pK_a	Intensities ratio[a]	R_{max}/R_{min}[b]	Q.Y.[c] Φ
4a	384,	1.681	522 (pH 9.0)	5.90	0.20 (pH 9.0)	~68	0.04 (pH 3.0)
	425 (pH 3.0)	1.884	645 (pH 3.0)		13.48 (pH 3.0)		0.02 (pH 9.0)
	550 (pH 9.0)	0.135					
4b	375,	2.190	557 (pH 9.0)	6.32	0.10 (pH 9.0)	~61	0.007 (pH 3.0)
	452 (pH 3.0)	2.045	686 (pH 3.0)		6.11 (pH 3.0)		0.002 (pH 9.0)
	588 (pH 9.0)	0.504					
4c	420 (br) (pH 3.0)	1.849	504 (pH 9.0)	5.50	0.11 (pH 9.0)	~143	0.07 (pH 3.0)
	550 (pH 9.0)	0.504	650 (pH 3.0)		15.76 (pH 3.0)		0.03 (pH 9.0)
4d	375,	0.938	524 (pH 9.0)	5.26	0.13 (pH 9.0)	~175	0.05 (pH 3.0)
	430 (pH 3.0)	0.841	673 (pH 3.0)		22.75 (pH 3.0)		0.02 (pH 9.0)
	555 (pH 9.0)	0.345					

[a] Intensities ratio of the emission peak with longer wavelength versus the peak with shorter wavelength.
[b] R_{max}=intensities ratio at pH 3.0; R_{min}=intensities ratio at pH 9.0.
[c] Fluorescence quantum yield (Q.Y.) was calculated relative to fluorescein (Φ=0.91 in 0.1 M NaOH).

100 MHz, respectively) in $CDCl_3$. High-resolution mass spectra were obtained on a Bruker Autoflex mass spectrometer (MALDI-TOF). Fluorescent emission spectra and UV–vis spectra were collected on a PTI luminescence lifetime spectrometer and a Cary UV-100 spectrometer, respectively. Unless specified, all fine chemicals were used as received.

4.2. 2,6-Diformyl-4-Phenylphenol (2d)

4-Phenylphenol (528 mg, 3.10 mmol) was reacted with 2 equiv hexamethylenetetramine (958 mg, 6.83 mmol) in trifluoroactetic acid (10 mL). The reaction mixture was refluxed at 150° C for 24 h under nitrogen atmosphere. Then the mixture was cooled to room temperature and stirred with 4 M HCl (10 mL) for 30 min. The mixture was extracted by dichloromethane (3×15 mL). The combined organic layers were washed successively by dilute hydrochloric acid, water, and saturated brine solution, followed by drying with anhydrous sodium sulfate. The organic solution was filtered and evaporated under vacuum to afford a crude residue that was purified by column chromatography (*n*-hexane/ethyl acetate 20:1) to yield pure **2d** (219 mg, 26.5% yield). H NMR (400 MHz, $CDCl_3$-d_1) 7.40, (tt, 1H, *J*=7.4, 1.3 Hz), 7.47 (t, 2H, *J*=7.2 Hz), 7.58 (dd, 2H, *J*=7.5, 0.6 Hz), 8.18 (s, 2H), 10.31 (s, 2H), 11.63 (s, 1H). Dialdehydes **2a**–**2c** were synthesized according to the literature procedure.[8]

Compound ***3b*** (obtained as pale yellow oil in 43% yield): H NMR ($CDCl_3$-d_1) δ (ppm): 3.83 (s, 3H), 7.21 (d, 1H, *J*=3.2 Hz), 7.37 (d, 1H, *J*=3.2 Hz) 8.40 (s, 1H), 10.13 (s, 1H), 10.61 (s, 1H). C NMR ($CDCl_3$-d_1) δ (ppm): 56.4, 116.4, 120.5, 121.4, 122.2, 125.1, 152.5, 154.4, 193.3.

Compound ***3c*** (obtained as pale yellow oil in 51% yield): H NMR ($CDCl_3$-d_1) δ (ppm): 7.80 (d, *J*=2.5 Hz), 7.90 (d, *J*=2.5 Hz), 8.27 (s, 1H), 10.10 (s, 1H), 11.02 (br s, 1H). C NMR ($CDCl_3$-d_1) δ (ppm): 117.1, 122.0, 132.3, 137.8, 138.6, 161.6, 148.8, 191.8.

Compound ***3d*** (obtained as pale yellow oil in 50% yield): H NMR ($CDCl_3$-d_1) δ (ppm): 7.37 (t, 1H, *J*=7.3 Hz), 7.46(t, 2H, *J*=7.8 Hz), 7.57 (d, 2H, *J*=7.1 Hz), 7.92 (d, 1H, *J*=2.3 Hz), 8.03 (d, 2H, *J*=1.8 Hz), 8.50 (s, 1H), 10.22 (s, 1H), 11.13 (br s, 1H). C NMR (MeOD-d_4) δ (ppm): 121.7, 124.3, 127.6, 128.6, 129.9, 130.1, 134.3, 134.5, 140.4, 149.1, 160.4, 193.6.

4.4. 6-(*tert*-Butyl)-1′,3′,3′-trimethylspiro[chromene-2,2′-indoline]-8-carbaldehyde oxime (4a)

To a solution of 5-(*tert*-butyl)-2-hydroxy-3-((hydroxyimino) methyl)benzaldehyde (20 mg, 0.09 mmol) and *N*-methyl-2,3,3-trimethylindolenine iodide (35 mg, 0.10 mmol) in anhydrous ethanol (10 mL), morpholine (2 mL) was added dropwise. The reaction mixture was refluxed at 60 °C for overnight. After being cooled to room temperature, part of solvent was removed under reduced pressure. Then the reaction mixture was diluted with water and extracted with ethyl acetate (3×10 mL). The combined organic

layers were dried by anhydrous sodium sulfate and filtered. The filtrate was evaporated under vacuum to afford a crude residue, which was purified by column chromatography (*n*-hexane/ethyl acetate 100:1) to yield product **4a** as purple oil (28 mg, 82% yield). H NMR ($CDCl_3$-d_1) δ (ppm): 1.16 (s, 3H), 1.28 (s, 12H), 2.71 (s, 3H), 5.70 (d, 1H, J=10.2 Hz), 6.50 (d, 1H, J=7.7 Hz), 6.81 (dd, 1H, J=7.2 Hz), 6.83 (d, 1H, J=10.2 Hz), 7.04 (d, 1H, J=7.1 Hz), 7.09 (d, 1H, J=1.9 Hz), 7.15 (dd, 1H, J=7.5, 7.7 Hz), 7.59 (d, 1H, J=1.9 Hz), 7.97 (br s, 1H), 8.18 (s, 1H). C NMR ($CDCl_3$-d_1) δ (ppm): 20.5, 25.9, 28.9, 31.4, 34.1, 51.8, 104.9, 106.8, 117.2, 118.8, 119.3, 120.0, 121.5, 122.5, 125.8, 127.6, 129.4, 136.4, 142.7, 145.6, 147.9, 150.4. HRMS (MALDI-TOF) for $C_{24}H_{28}N_2O_2$ calcd 377.2223 ($M+H^+$), found, 377.2230.

Using the same procedure, **4b**, **4c**, and **4d** were prepared.

Compound ***4b*** (as purple oil in 43% yield): H NMR ($CDCl_3$-d_1) δ (ppm): 1.16 (s, 3H), 1.28 (s, 3H), 2.71 (s, 3H), 3.76 (s, 3H), 5.76 (d, 1H, J=10.2 Hz), 6.50 (d, 1H, J=7.7 Hz), 6.69 (d, 1H, J=3.0 Hz), 6.81 (d, 1H, J=10.2 Hz), 6.84 (d, 1H, J=3.0 Hz), 7.04 (d, 1H, J=6.8 Hz), 7.15 (m, 2H), 7.51 (br s, 1H), 8.15 (s, 1H). C NMR ($CDCl_3$-d_1) δ (ppm): 20.5, 26.0, 28.9, 51.8, 55.8, 104.6, 106.8, 109.1, 115.4, 118.3, 119.3, 120.3, 121.3, 121.5, 127.6, 128.9, 136.4, 145.3, 147.0, 147.9, 152.9.

Compound ***4c*** (as purple oil in 68% yield): H NMR ($CDCl_3$-d_1) δ (ppm): 1.16 (s, 3H), 1.27 (s, 3H), 2.71 (s, 3H), 5.77 (d, 1H, J=10.3 Hz), 6.51 (d, 1H, J=7.7 Hz), 6.79 (d, 1H, J=10.3 Hz), 6.86 (dd, 1H, J=7.2, 7.4 Hz), 7.05 (dd, 1H, J=7.2, 7.4 Hz), 7.14–7.19 (m, 2H), 7.52 (br s, 1H), 7.71 (d, 1H, J=2.4 Hz), 8.06 (s, 1H). C NMR ($CDCl_3$-d_1) δ (ppm): 20.4, 25.9, 28.9, 29.7, 52.1, 105.4, 106.9, 112.3, 119.6, 120.1, 121.3, 121.5, 127.8, 128.1, 128.3, 130.6, 136.1, 144.1, 147.6, 151.4. HRMS (MALDI-TOF) for $C_{20}H_{19}BrN_2O_2$ calcd 401.0684 ($M+H^+$), found, 401.0669.

Compound ***4d*** (as purple oil in 50% yield): H NMR ($CDCl_3$-d_1) δ (ppm): 1.18 (s, 3H), 1.31 (s, 3H), 2.74 (s, 3H), 5.77 (d, 1H, J=10.2 Hz), 6.52 (d, 1H, J=7.7 Hz), 6.84 (dt, 1H, J=7.5, 0.8 Hz), 6.91 (d, 1H, J=10.2 Hz), 7.05 (dd, 1H, J=7.2, 7.4 Hz), 7.16 (dd, 1H, J=7.4, 7.6 Hz), 7.22–7.30 (m, 2H), 7.38 (t, 2H, J=7.3 Hz), 7.53 (d, 2H, J=7.1 Hz), 7.85 (d, 1H, J=2.2 Hz), 8.20 (s, 1H). C NMR (DMSO-d_6) δ (ppm): 20.0, 25.5, 28.6, 51.5, 79.1, 104.8, 106.9, 118.8, 119.2, 119.7, 120.2, 121.4, 122.9, 126.1, 126.4, 127.1, 127.5, 128.9, 129.2, 132.3, 136.1, 139.4, 141.7, 147.73, 147.6, 151.0. MALDI-TOF $[M+H]^+$ calculated for $C_{26}H_{25}N_2O_2$: 397.1910; found: 397.1929. HRMS (MALDI-TOF) for $C_{26}H_{25}N_2O_2$ calcd 397.1910 ($M+H^+$), found, 397.1929.

Acknowledgements

The work was supported by a grant from the Research Committee of Hong Kong Baptist University (FRG2/11-12/121).

Supplementary data

Supplementary data associated with this article can be found in the online version, at http://dx.doi.org/10.1016/j.tet.2013.05.023.

References and notes

1. (a) Chen, X.; Pradhan, T.; Wang, F.; Kim, J. S.; Yoon, J. *Chem. Rev.* **2012**, *112*, 1910–1956; (b) Nolan, E. M.; Lippard, S. J. *Chem. Rev.* **2008**, *108*, 3443–3480.
2. (a) Duke, R. M.; Veale, E. B.; Pfeffer, F. M.; Kruger, P. E.; Gunnlaugsson, T. *Chem. Soc. Rev.* **2010**, *40*, 2222–2235; (b) Martnez-Manez, R.; Sancenon, F. *Chem. Rev.* **2003**, *103*, 4419–4476.
3. (a) Zhou, Y.; Yoon, J. *Chem. Soc. Rev.* **2012**, *41*, 52–67.
4. (a) Urano, Y.; Asanuma, D.; Hama, Y.; Koyama, Y.; Barrett, T.; kamiya, M.; Nagano, T.; Watanabe, T.; Hasegawa, A.; Choyke, P. L.; Kobayashi, H. *Nat. Med.* **2009**, *15*, 104–109; (b) Tang, B.; Yu, F.; Li, P.; Tong, L.; Duan, X.; Xie, T.; Wang, X. *J. Am. Chem. Soc.* **2009**, *131*, 3016–3023; (c) Lei, J.; Wang, L.; Zhang, J. *Chem. Commun.* **2010**, 8445–8447; (d) Zhou, X.; Su, F.; Lu, H.; Senechal-Willis, P.; Tian, Y.; Johnson, R. H.; Meldrum, D. R. *Biomaterials* **2012**, *33*, 171–180; (e) Hutt, J. T.; Jo, J.; Olasz, A.; Chen, C.-H.; Lee, D.; Aron, Z. D. *Org. Lett.* **2012**, *14*, 3162–3165.
5. (a) Santra, M.; Roy, B.; Ahn, K. H. *Org. Lett.* **2011**, *13*, 3422–3425; (b) Chen, W.-H.; Xing, Y.; Pang, Y. *Org. Lett.* **2011**, *13*, 1362–1365; (c) Yang, X.; Guo, Y.; Strongin, R. M. *Angew. Chem., Int. Ed.* **2011**, *50*, 10690–10693.
6. (a) Shao, N.; Jin, J. Y.; Wang, H.; Zhang, Y.; Yang, R. H.; Chan, W. H. *Anal. Chem.* **2008**, *80*, 3466–3475; (b) Zhu, J.-F.; Chan, W.-H.; Lee, A. W. M. *Tetrahedron Lett.* **2012**, *53*, 2001–2004; (c) Shao, N.; Wang, H.; Gao, X.; Yang, R. H.; Chan, W. H. *Anal. Chem.* **2010**, *82*, 4628–4636; (d) Shao, N.; Jin, J.; Wang, H.; Zeng, J.; Yang, R. H.; Chan, W. H. *J. Am. Chem. Soc.* **2010**, *132*, 725–736.
7. Wojtyk, J. T. C.; Wasey, A.; Xiao, N.-N.; Kazmaier, P. M.; Hoz, S.; Yu, C.; Lemieux, R. P.; Buncel, E. *J. Phys. Chem. A* **2007**, *111*, 2511–2516.
8. Lindoy, L. F.; Meehan, G. V.; Svenstrup, N. *Synthesis* **1998**, 1029–1032.
9. Shao, N.; Zhang, Y.; cheung, S.; Yang, R. H.; Chan, W. H.; Mo, T.; Li, K. A.; Liu, F. *Anal. Chem.* **2005**, *77*, 7294–7303.
10. Henary, M. M.; Fahrni, C. J. *J. Phys. Chem. A* **2002**, *106*, 5210–5220.